

# Numerical Modeling of Excimer Laser Curved Surface Ablation

ICOMM  
2013  
No. 44Vivek Garg<sup>1</sup>, Deepak Marla<sup>2</sup>, Ishan Saxena<sup>3</sup> and Suhas S. Joshi<sup>4</sup><sup>1</sup>Vivek Garg, Dept. of Mechanical Engineering, IIT Bombay, India; vivekgarg@iitb.ac.in<sup>2</sup>Deepak Marla, Dept. of Mechanical Engineering, IIT Bombay, India; deepakmarla@iitb.ac.in<sup>3</sup>Ishan Saxena, Dept. of Mechanical Engineering, Northwestern University, U. S.; ishan@u.northwestern.edu<sup>4</sup>Suhas S. Joshi, Dept. of Mechanical Engineering, IIT Bombay, India; ssjoshi@iitb.ac.in \*

**Key Words:** Laser ablation, curved surface ablation, finite element modeling, profiled path approach, beam path approach

## ABSTRACT

Laser ablation has been widely used in the fabrication of miniature parts. The technique is also used in the fabrication of micro lens or micro-curved surfaces which find potential applications in various optical, bio- medical, electronics, MEMS applications. This work presents development of two novel techniques employing profile path approach and beam profile approach for fabrication of curved surfaces by Excimer laser ablation. Laser ablation is widely used for their fabrication on account of its exceptional capabilities. In this paper, a two-dimensional finite element model is developed to predict temperature distribution and ablation depth in a laser ablation process. A correlation between the incident laser fluence and depth of the ablated crater is analytically generated based on the FEM model. Using this correlation, the profiles of the surface ablated using profile path and beam path approach is predicted based on a finite element model incorporating the pulse variation in profile path approach and spatial variation of intensity of the incident beam in the beam path approach. Modeling of various profiles like flat, circular, Gaussian and other is also presented. An attempt has been made to validate the proposed techniques experimentally.

## INTRODUCTION

Laser ablation is an important field of applied and fundamental research over past few decades due to growing need of miniaturisation, high speed and precise micromachining abilities, applications in the fields of manufacturing, electronics, medicines etc. Laser ablation is the process of material removal from a target surface by absorption of incident laser fluence. Target surface is melted and vaporised by the laser fluence falling on the surface. Distinct advantage of laser ablation as compared to other conventional material removal process lies in the fact that ablation is strictly confined to the very small area that absorbs the energy, allowing it to use in micromachining applications.

Interaction of laser with polymers is quite complicated, which involves several mechanisms. Interaction between the laser beam and materials has not been clarified in every detail so far in spite of the important field of research and wide use of laser technologies, especially in the case of polymers.

Laser ablation of polymers was first reported nearly simultaneously by two groups in 1982 [1, 2]. A dynamic model was reported by moving irradiated interface [3]. A model for excimer laser etching of polymers considering the dependence of etched depth per pulse on the incident radiation fluence was proposed [4]. UV laser ablation of polymers was believed to be a pure photothermal effect originally [5], however evidence was obtained that bond breaking in polymers is significant and a photochemical nature of laser ablation was considered [6]. A combined photochemical and photothermal model for polymer ablation was considered later [7]. Models were developed to understand the phenomenon of ablation in polymers by considering the photochemical mode of ablation of polymers by taking into account polymer degradation due to bond breaking induced by thermal effects [8]. Dynamics of absorption of radiation by the plasma in pulsed laser ablation have also been explained in the literature [9].

Ablation rate of the laser depends on temperature, the material properties and accumulation of heat in the work material. In consequence, to control the laser processing, thermal distribution of the sample has to be determined, which can be made by modeling of the laser ablation. By using such modeling tool, proper laser parameters can be determined easier and faster. However, in spite of lot of research, effect of these parameters has not been satisfactorily clarified. Thermal effects, photochemical and other phenomena still exist and so the modeling of laser ablation is a very specialised problem. Geometry of the domain under investigation varies during the simulation, because laser pulses remove material from the sample. Laser ablation of PMMA for a single pulse in number of substeps is modelled and matched with experimental and literature values.

A number of fabrication methods like Electron beam Lithography [10], hot embossing [11], using elastomeric molds of PDMS [12], an ink jet printing [13], gray scale lithography [14], circular scanning method [15], gray scale diffractive mask based phase shifting gratings [16] have been reported and employing pulsed laser ablation for creating desired profiles. However, most of the curved surface fabrication processes mentioned above have a limitation in the sense that they fail to produce exact surface profile. Therefore, there is still a need for a simpler fabrication process to accurately produce the desired lens shape. In this work, laser ablation is considered as a possible alternative step to fabricate the curved

\* corresponding author

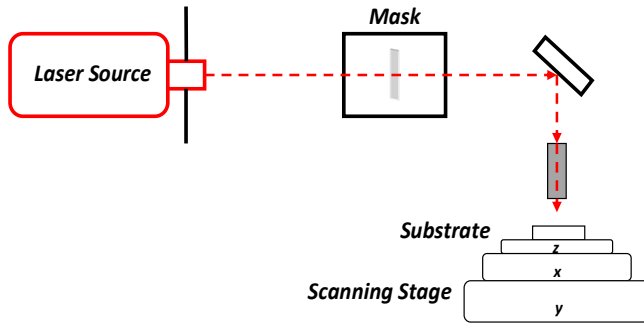


Fig. 1: A typical excimer laser setup employing mask and a scanning stage

surfaces. It utilizes pulsed lasers of short wavelength such as ArF(193 nm), KrF (248 nm), XeCl (308 nm), and XeF (351 nm). The laser pulses usually have high pulse energy and short pulse duration, in the range of 1- 100 nanoseconds. A typical excimer laser micromachining setup is shown in Fig. 1. The system may also be equipped with an optical projection system, which modulates the laser beam pattern with a photo-mask. The setup may also use a servo controlled mechanical scanning stage.

The fabrication is based on two techniques namely, beam path approach and profile path approach. The former technique is based on systematic modification of the laser intensity profile to get the desired curved surface, while the latter technique uses different number of pulses along the surface without changing the spatial intensity profile. Both the techniques are based on the idea of varying the incident laser energy spatially to generate non-uniform ablation depth. In this work, a two-dimensional finite element model is developed to simulate the curved surface profiles by spatial variations in laser intensity profiles. A qualitative analysis of the incident laser intensity profile and the resultant ablation depth profile is presented for a number of profiles.

#### CURVED SURFACE ABLATION

The key to the technique for laser precision ablation of three-dimensional (3D) intricate microstructures is its ability to operate a laser beam with a proper beam shape, intensity, and wavelength to remove a required amount of material from a pre-defined location in a controllable manner. A precise knowledge of the ablation rate, especially the effects of major operating parameters, including fluence, pulse duration, and pulse number on the ablation rate is essential to achieve the precision ablation of complicated structures. Ablation depth for  $N$  number of pulses falling on the substrate can be written as [17],

$$h_e = \left( \frac{N}{\alpha} \right) \ln \left[ \frac{F}{F_{th}} \right], \text{ if } F > F_{th} \quad (1)$$

Where,  $h_e$  is the ablation depth,  $\alpha$  is the effective absorption coefficient,  $F$  is incident fluence and  $F_{th}$  is threshold fluence. Mathematically, the ablation depth,  $h_e$ , can be represented by a function of the Cartesian coordinates,  $(x, y)$ . To have an arbitrarily curved surface,  $h_e(x,y)$ , either the laser pulse ( $N$ ) or the fluence ( $F$ ) has to be a function of  $x$  and  $y$ . The following two approaches for curved surface ablation are presented in

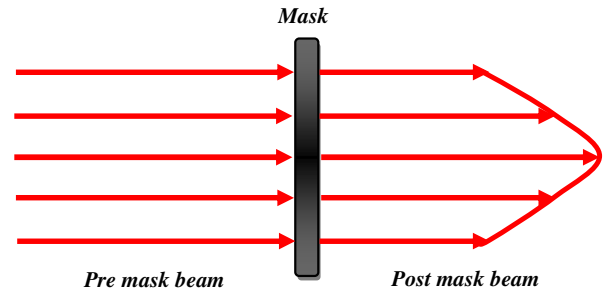


Fig. 2: Modification of beam intensity profile using mask

this work:

- A. Beam Path Approach
- B. Profiled Path Approach

The first approach changes the beam intensity profile over its cross section by employing a mask in the beam path and generates the desired profile. The second approach approximates the ablated surface by multiple exposures and moving the beam along the specific path.

#### BEAM PATH APPROACH

Ablation depth of the curved surface ( $h_e$ ) can also be achieved using a projection excimer laser ablation system by adequately controlling the magnitude of the fluence ( $F$ ) as indicated by,

$$h_e = \left( \frac{N}{\alpha} \right) \ln \left[ \frac{F(x, y)}{F_{th}} \right] \quad (3)$$

In order to control the shape of ablated crater, the intensity variation of the incident beam across its cross section needs to be controlled. It is based on a simple but very constructive idea by changing the beam profile in accordance with the profile required. A gray scale mask can be used for altering the beam profile [16]. A two dimensional finite element model has been developed and a number of simulations in this study have been done for various laser fluence profiles like flat, Gaussian, parabolic, exponential and others to simulate the laser ablated profiles by beam path approach. Fig. 2 shows the modification of beam intensity profile employing a mask by beam path approach.

#### PROFILED PATH APPROACH

Ablation depth of the curved surface ( $h_e$ ) can be achieved using a projection excimer laser ablation system by adequately controlling the number of laser pulses ( $N$ ) as indicated by,

$$h_e = \left( \frac{N(x, y)}{\alpha} \right) \ln \left[ \frac{F}{F_{th}} \right] \quad (2)$$

This approach makes use of a simple circular hole as beam aperture for the excimer laser and the translation stage carrying the polymer substrate, capable of making movements. All the laser related parameters like the pulse energy and the pulse frequency of the laser remain invariant during the process. While the excimer laser is firing pulses, the translation stage makes subsequent scans with different radii and speeds.

By careful choice of both radius and number of pulses, an arbitrary desired curved surface can be obtained. Both, convex and concave profiles can be obtained employing this approach.

**FINITE ELEMENT MODELING**

A finite element model is developed to simulate the laser ablation process with different laser intensity profiles. Commercial software ANSYS 13 has been used in the simulation [2]. Due to symmetry along the center of the beam, only half of the target is simulated. Considering an incremental time step of 1 ns over a pulse duration time of 20 ns, this time dependent problem has been solved sequentially. Ablation is assumed to occur, when the temperature of an element is higher than the boiling point temperature ( $T_b$ ) at the end of a particular sub-step. The output of the last time step is taken as input to the next time step. Phase change effects are taken into account by considering the latent heat of vaporization (L) in the model. Fig. 3 shows the modeling approach adopted in this section.

**TARGET GEOMETRY**

The target geometry used for simulation is given in Fig. 4. The target is taken to be rectangular in shape with dimension of  $18 \mu\text{m} \times 6 \mu\text{m}$ . Only half of the target is simulated because of the axial symmetry of the problem. Moreover, only part of the simulated region is irradiated in order to account for the lateral heat losses to the non-irradiated part of the sample. The size of each element is  $50\text{nm} \times 50\text{nm}$ . The element used for the analysis is PLANE 55. The element has four nodes with single degree of freedom, temperature, at each node. The element can be applied for 2D, axi-symmetric, steady state or transient thermal analysis.

**ASSUMPTIONS**

The following assumptions are considered in the model:

- A 2D heat conduction equation is assumed.
- Heat source distribution is assumed to be of temporal Gaussian profile and constant over beam cross section.
- Since the molten volume of the target material is very low in laser ablation process, convective heat transfer effects are not considered.

**HEAT FLUX AND BOUNDARY CONDITIONS**

The temperature distribution induced in a material due to heat source is given by 2D heat conduction equation as [18],

$$\rho(T)c_p(T) \frac{\partial T(x, z, t)}{\partial t} = \nabla [k(T) \nabla T(x, z, t)] + Q(z, t) \quad (3)$$

where,  $\rho$ ,  $C_p$ ,  $k$  are the mass density, specific heat at constant pressure and thermal conductivity of the target material respectively.  $(x, z)$  are the space coordinates;  $z$  being normal to the surface. The source term  $Q(z, t)$  represents the laser energy absorbed by the sample and is given by,

$$Q(z, t) = I_s(t)(1 - R)\exp(-Bz) \quad (4)$$

where,  $R$  and  $B$  are the reflectivity and the absorption

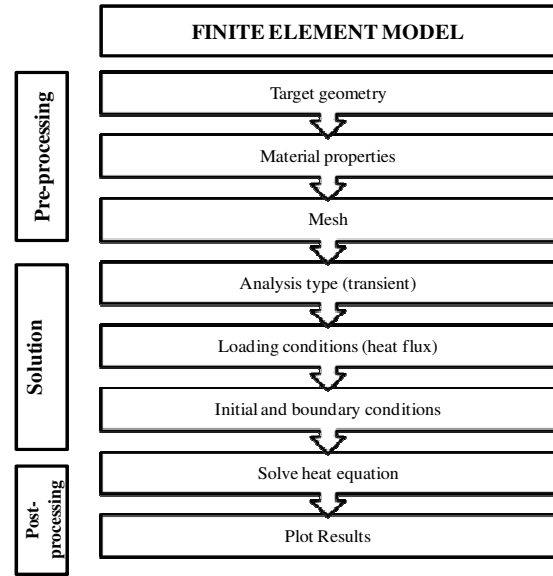


Fig.3: Layout of modeling approach

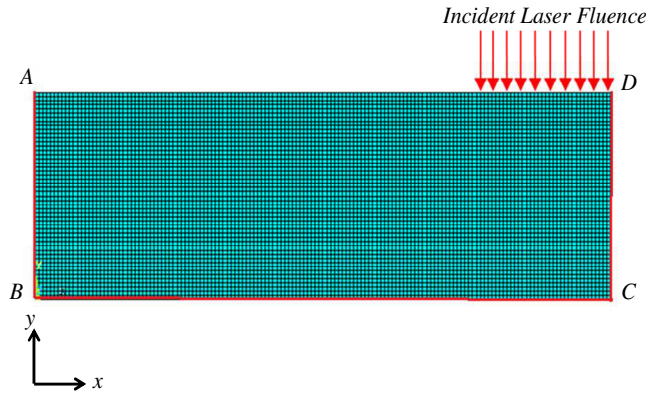


Fig. 4: Target geometry in the finite element model

coefficient of the target material respectively.  $I_s(t)$  is the temporal laser irradiance at the sample surface. As the heating occurs, there is a phase change from solid to liquid and liquid to vapor. The model takes this phenomenon into account by just adding the latent heat of fusion and latent heat of vaporization whenever the target element reaches melting point, and vaporization point respectively.

$$\rho(T)c_p(T) \frac{\partial T(x, z, t)}{\partial t} - k(T) \frac{\partial^2 T}{\partial z^2} = Q(z, t), \quad T < T_m \quad (5)$$

The above condition implies that the incident laser energy onto the surface is conducted into the work piece, when target temperature is less than its melting temperature.

$$\rho(T)c_p(T) \frac{\partial T(x, z, t)}{\partial t} - k(T) \frac{\partial^2 T}{\partial z^2} = -L + Q(z, t), \quad T > T_m \quad (6)$$

This implies that when the target temperature exceeds its melting point, latent heat (L) comes into picture. The boundary conditions in Fig. 4 are given by following equations:

$$T(x, t)|_{z=0} = T_0 \quad (\text{along boundary BC in Fig. 4}) \quad (7)$$

$$T(z, t)|_{x=0} = T_0 \quad (\text{along boundary AB in Fig. 4}) \quad (8)$$

$$-k(T) \frac{\partial T}{\partial x} \Big|_{x=18\mu m} = 0 \text{ (along boundary CD in Fig. 4)} \quad (9)$$

Initially, the temperature of the body is equal to ambient temperature:  $T(z,0) = T_0$  (10)

In the present model, radiation heat loss occurs both during the pulse on-time and pulse off-time. The top surface of the target is exposed to ambient due to which radiation heat transfer takes place, while the heat transfer inside the target material occurs by conduction. The radiation heat transfer is given by:

$$Q_{rad} = A \epsilon \sigma (T_s^4 - T_o^4) \quad (11)$$

where, A is the surface area in m<sup>2</sup>, ε is emissivity of the target, σ is Stefan-Boltzman constant, T<sub>s</sub> is surface temperature and T<sub>o</sub> is ambient temperature.

**ELEMENT REMOVAL TECHNIQUE**

The temperature of each element is calculated at the end of each substep. If the element temperature exceeds the melting temperature, the ablation is assumed to occur and the elements above melting temperature will be removed. Material removal in ANSYS is achieved through element birth and death technique, using the ‘ekill’ commands to deactivate the elements. All the properties associated with the deactivated elements are set to zero, such as element loads, specific heat, thermal conductivity etc. Ablation position is easily identified by killed elements and their position. Having gained an insight into the ablation phenomenon and knowing the ablation depth per pulse for different fluences, we will now investigate fabrication approach adopted for curved surface ablation in polymers by excimer laser ablation technique.

**CURVED SURFACE ABLATION MODELING**

Simulations based on the curved surface ablation model developed in the previous section are run with different loading conditions. Keeping all the conditions i.e. laser fluence, pulse time and target material unchanged, the laser beam intensity profile has been modified to different profiles to achieve curved surface ablation. The plots of variation of laser intensity across the beam cross section for various profiles considered are as shown in Fig. 5.

The profile of the laser radiation after passing through the grey scale mask is directly dependent on its opacity function. Therefore, the desired intensity profile can be obtained by choosing the opacity function of the gray scale mask. As there exist no direct correlation between the laser intensity profile and the ablated surface profile, a number of laser intensity profiles are considered in the simulation to study and establish a co-relation between the two. Different profiles of laser intensity are considered in the model keeping the laser fluence constant. The profiles include:

- i. Top-hat (uniform beam),  $I = I_0$
- ii. Exponential,  $I = I_0 \exp(-x)$
- iii. Gaussian,  $I = I_0 \exp(-0.5(x/\sigma)^2)$
- iv. Triangular,  $I = I_0(1-x)$
- v. Parabolic,  $I = I_0(1-x^2)$

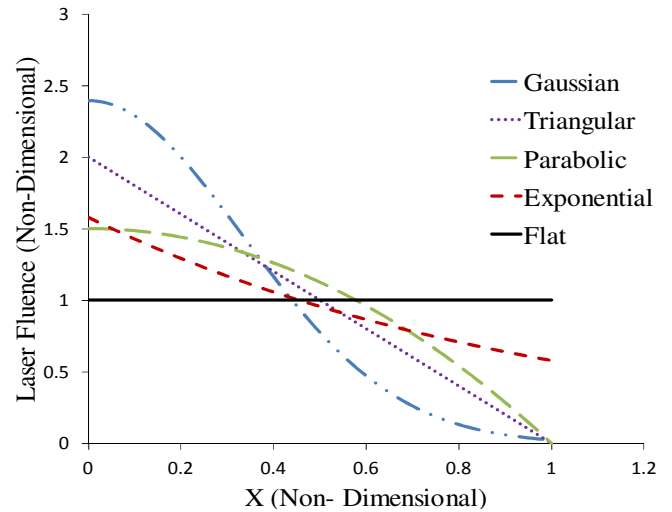


Fig. 5: Modification of laser fluence profile for curved surface laser ablation for a fixed fluence of 1J/cm<sup>2</sup>

The profiles represent the variation of intensity for half the target considered for simulation in this analysis. The plots are non-dimensionalized on both the axes. On the y-axis is plotted the intensity profile, non-dimensionalized with the intensity of top-hat (uniform beam). While the x-axis represents width of the target non-dimensionalized with half the width of the beam. The edge of the beam is taken as '1' while the origin is fixed at the center of the beam.

**RESULTS**

**SINGLE PULSE ABLATION**

In the initial analysis, single pulse simulations for un-modified beam has been carried out. The target surface is heated with single pulse of flat spatial profile and with laser fluence varying in the range from 1 J/cm<sup>2</sup> to 2.5 J/cm<sup>2</sup>. Fig. 7 shows the simulation results for ablation depths for single pulse measured. Boiling point of PMMA is 327 °C. The element birth and death process is employed to simulate material removal. The total pulse duration of 20 ns is divided into 20 sub-steps and after each sub-step all the elements with temperatures exceeding the boiling temperature are deleted. Fig. 6(a-d) shows the simulated profiles of ablation for the unchanged beam at four different laser fluences for a single pulse. The depth of ablation obtained at different fluences is tabulated in Table 1. The four profiles in Fig. 6(a-d) clearly indicate that for an unmodified, uniform beam along the cross-section, the profile of the ablated surface is nearly flat except at the edges of the beam cross-section. The profile at the edge of beam cross-section is circular because of the heat conduction in the lateral (perpendicular to the depth) direction.

Table 1: Simulated ablation depth per pulse

Laser fluence (J/cm <sup>2</sup> )	1.0	1.5	2.0	2.5
Ablation depth per pulse (μm)	1.16	1.24	1.28	1.36



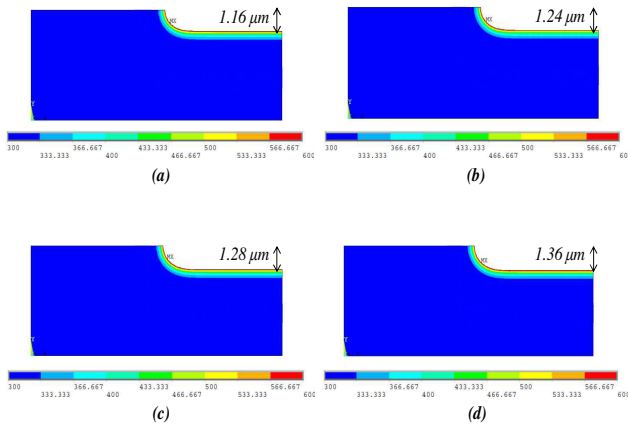


Fig. 6: Ablation depth for laser fluence of (a) 1 J/cm<sup>2</sup>, (b) 1.5 J/cm<sup>2</sup>, (c) 2 J/cm<sup>2</sup>, (d) 2.5 J/cm<sup>2</sup>

**CURVED SURFACE ABLATION**

The simulation results of laser ablation for the above mentioned laser intensity profiles for a fluence of 1 J/cm<sup>2</sup> is shown in Fig. 7(a-d): (a) flat (b) Gaussian (c) parabolic and (d) exponential with beam width = 6σ. A comparative study of the profiles of ablated surfaces are shown in Fig. 8. The various profiles obtained are compared with that of the simulation result considering top-hat (uniform beam). The plots in Fig. 8 clearly indicate the variation of surface profile for different profiles of laser intensities, although the ablation depths obtained are nearly the same. A better view of the comparison of these four profiles is presented in Fig. 3 that clearly shows the variation in resultant ablation profiles. A co-relation between the incident laser profiles can be obtained using such simulations that can further be used in fabrication of desired curved surfaces.

**EXPERIMENTAL VALIDATION**

Experiments are carried out for a range of laser fluences to validate the simulation results obtained. A Lamda Physik, 248nm KrF excimer laser setup equipped with a MicroLAS beam projection system has been used. A beam delivery system was used to project the laser beam radiated by the source onto the substrate. The beam delivery setup employs a homogenizer 2D array which makes the intensity of the beam constant over its cross section. Thus the simulation results of

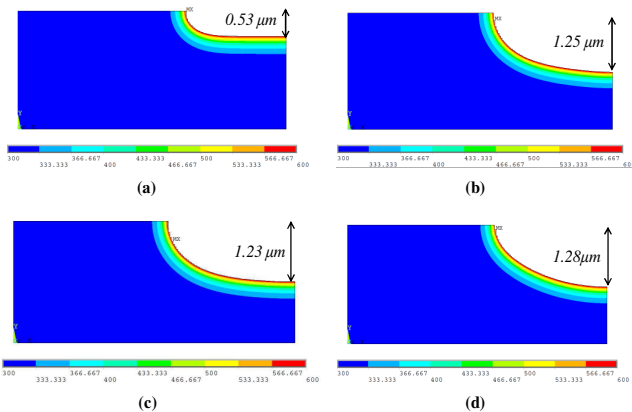


Fig. 7: Simulation results for curved surface laser ablation: (a) flat, (b) Gaussian, (c) parabolic and (d) exponential

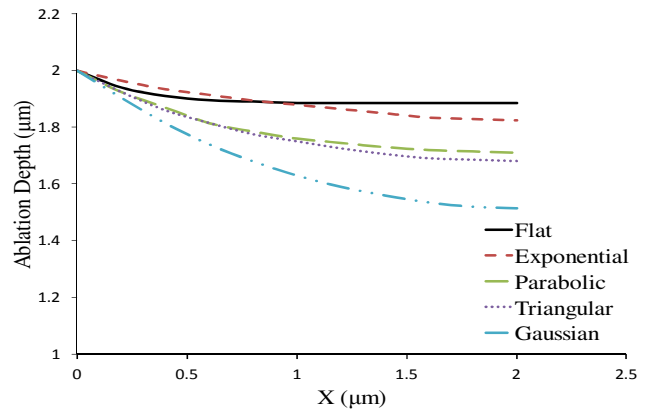


Fig. 8: Comparison of simulated profiles for curved surface laser ablation

flat top profile of incoming laser fluence are validated by the experiments. Experimental setup used for laser ablation validation is shown in Fig. 9. The technical specifications of the experimental ablation setup are presented in Table 2. Using this set-up, PMMA substrate was ablated for four different values of laser fluence of 1 J/cm<sup>2</sup>, 1.5 J/cm<sup>2</sup>, 2 J/cm<sup>2</sup> and 2.5 J/cm<sup>2</sup>. The aim of the experiments was to calculate the ablated depth per pulse of the incident radiation. For ease of depth measurement, multiple pulses were fired and the total ablated depth was measured. Each experiment was carried out at pulse frequency f = 10Hz and the pulses were fired for a time of t = 40s. Based on the experiments, an average value of ablation depth was measured for different fluences, tabulated in Table 3.



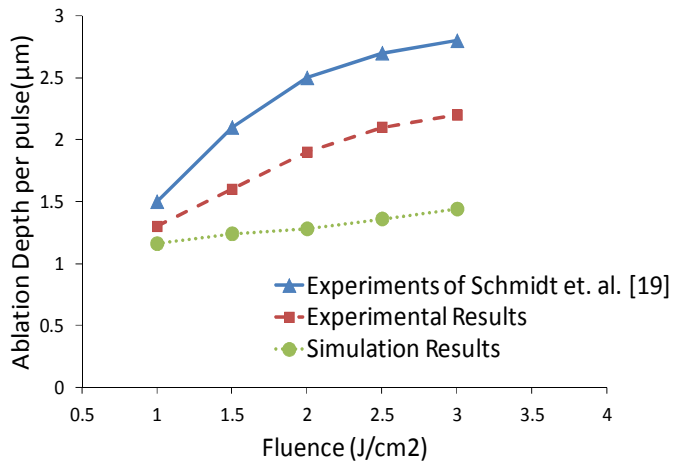
Fig. 9: Photographic view of the experimental set-up

Table 2: Technical specifications of experimental setup

Wavelength	248nm(KrF)
Max. energy	650mJ
Pulse duration	20ns
Repetition rate (frequency)	1-50 Hz
Beam size	15mm X 15mm
XYZ stage accuracy	1μm
Resolution	3 micron feature

**Table 3: Experimental ablation depth per pulse**

Laser fluence (J/cm <sup>2</sup> )	1	1.5	2	2.5
Ablation depth per pulse (μm)	1.30	1.60	1.90	2.10

**Fig. 10: Comparison of simulation results with experimental values and data from literature**

#### COMPARISON WITH SIMULATION AND LITERATURE

The experimental results are compared with the simulation results of previous section and also to typical depth per pulse values for polymer ablation available in literature [19]. The literature values have been evaluated using a numerical model for ablation for uniform beam cross-section. Fig. 10 shows the comparison of all results.

The comparison has been done only of the uniform (flat) profile to establish the accuracy of the model. FEM generated values underestimate the ablation depth. For lower energy the deviation is significant, however for high energy, ablation depth per pulse values of the developed FEM model are within 10% of the experimental values. The experimental values agree fairly well with the literature values [19].

#### CONCLUSIONS

Laser ablation using beam path approach and profiled path approach are two potentially viable techniques for fabrication of desired surface profiles.

A correlation between intensity of the incident beam and the ablated depth can be established using the developed numerical model. This correlation can be used to derive the gray-scale mask opacity function to generate the desired surface profile of the curved surfaces.

The loading flux conditions in the developed numerical model were modified using the varying profiles. The generated surface profile matches closely to the desired curved surface. The proposed techniques can be employed to generate surfaces of any arbitrary shapes, on account of its flexibility.

Simulation results of the developed finite element model lies within the accuracy of 10% at lower fluence, however results shows a significant disagreement at higher fluence due to

photothermal modeling only. Experimental results agree well with theoretical models that consider both photochemical and photothermal modes of ablation as compared to finite element model that considers only photothermal ablation. This indicates that both these modes play a significant role in ablation of polymers.

#### REFERENCES

- [1] R. Srinivasan, et al., "Self-developing photoetching of poly(ethylene terephthalate) films by far-ultraviolet excimer laser radiation", *Applied Physics Letters*, 1982; 41(6): 576–578.
- [2] Y. Kawamura et al., "Effective deep ultraviolet photoetching of polymethyl methacrylate by an excimer laser", *Applied Physics Letters*, 1982; 40(5): 374–375.
- [3] S. Lazare et al., "Ultraviolet Laser Photoablation of Polymers: A Review and Recent Results", *Laser Chemistry*, 1989; 10(1): 25–40.
- [4] V. Srinivasan et al., "Excimer laser etching of polymers", *J. Appl. Phys.*, 1986; 59(11): 3861–3867.
- [5] L. Galantucci. "Excimer Laser Cutting: Experimental Characterization and 3D Numerical Modelling for Polyester Resins", *CIRP Annals*, 1998; 47(1): 141–144.
- [6] Wu, B., and Shin, Y. C., 2006. "Modeling of nanosecond laser ablation with vapor plasma formation", *J. Appl. Phys.*, 99(8): 084310.
- [7] N. Bityurin et al., "Models for laser ablation of polymers", *Chemical reviews*, 2003; 103(2): 519–552.
- [8] N. Arnold et al., "Laser-induced thermal degradation and ablation of polymers: bulk model", *Applied Surface Science*, 1999; 138–139: 212–217.
- [9] D. Marla et al., "Critical assessment of the issues in the modeling of ablation and plasma expansion processes in the pulsed laser deposition of metals", *J. Appl. Phys.*, 2011; 109(2): 021101.
- [10] T. Fujita et al., "Fabrication of micro lenses using electron-beam lithography", *Optics letters*, 1981; 6(12): 613–615.
- [11] X. J. Shen et al., "Microplastic embossing process: experimental and theoretical characterizations", *Sensors and Actuators A: Physical*, 2002; 97–98: 428–433.
- [12] Shin, T. K., Ho, J. R., and Cheng, J. W. J., 2004. "A New Approach to Polymeric Microlens Array Fabrication Using Soft Replica Molding". *IEEE Photonics Technology Letters*, 16(9), 2078–2080.
- [13] A. Christopher, "Microlens array fabrication via microjet printing technologies", *J. Appl. Phys.*, 2007; 28: 2–7.
- [14] C. McKenna et al., "Maskless Direct Write Grayscale Lithography for MEMS Applications", *UGIM*, 2010; 18: 1–4.
- [15] K. Naessens et al. "Laser ablation based technique for flexible fabrication of microlenses in polymer materials". *Proceedings of SPIE*, 2002; 124–127.
- [16] A. Braun et al., "Diffractive gray scale masks for excimer laser ablation", *Applied Surface Science*, 2002; 186: 200–205.
- [17] V. Srinivasan et al., "Excimer laser etching of polymers", *J. Appl. Phys.*, 1986; 59: 3861–3867.
- [18] N. A. Vasantgadkar et al., "A finite element model to predict the ablation depth in pulsed laser ablation", *Thin Solid Films*, 2010; 519: 1421–1430.
- [19] H. Schmidt et al., "Ultraviolet laser ablation of polymers: spot size, pulse duration, and plume attenuation effects explained", *J. Appl. Phys.*, 1998; 83: 5458